

Size effect on microstructure and tensile properties of Sn3.0Ag0.5Cu solder joints

Shaobin Wang¹ · Yao Yao¹ · Xu Long¹

Received: 14 May 2017 / Accepted: 12 August 2017 / Published online: 19 August 2017
© Springer Science+Business Media, LLC 2017

Abstract In the current study, the size effect on microstructure and tensile property of Sn3.0Ag0.5Cu (SAC305) solder joint is investigated. Experiments were performed to solder joints with thickness from 50 μm to 2 mm. The intermetallic compound (IMC) growth rate of solder joints is found to be dependent on the size of solder joints. After soldering procedure, the IMC of smaller size solder joints is thinner than that of larger size solder joints. It is also found that the average grain size of IMC increases with decreasing of the joint size. To better understand the difference of IMC growth during solid-state and liquid-state thermal aging, experiments were performed at 210 and 300 $^{\circ}\text{C}$, respectively. IMC thickness of solder joints after 210 and 300 $^{\circ}\text{C}$ of thermal aging was measured. It is found that the size effect on IMC growth rate at solid-state and liquid-state is different. The IMC growth rate of smaller size solder joints is higher than larger size solder joints under solid-state thermal aging. Under liquid-state reaction, the IMC growth rate of smaller size solder joints is slower. ‘H’ type and hexagonal prism of Cu_6Sn_5 were observed in 2 and 1 mm thickness size solder joint, respectively. Fewer Cu_6Sn_5 prism was found in 50 μm thickness solder joints. Tensile strengths of solder joints with different sizes were measured. The solder joints showed ductile to brittle fracture transition with the decreasing of joints thickness. The H -field fracture criterion is employed to predict the tensile strength of Sn3.0Ag0.5Cu solder joints with different thickness.

1 Introduction

The development of 3D integrated circuit packaging technology leads the solder interconnect to the size range of sub-50 μm , which brings the concern of size effect on solder joint reliability [1, 2]. Mechanical and thermal properties are the basis of solder joint reliability, which vary with the dimension of solder joints. Thus the long-term reliability of electronic products demands an exhaustive understanding of the differences between various dimensional solder interconnects. Under thermal aging cycle or drop impact loading, damage could initiate at interfacial intermetallic compound (IMC) layer due to its relatively brittle property. Thus, the size effect on microstructure such as IMC layer of solder joints is one of the primary problems to explore with respect to solder reliability. Many researches have been performed to investigate the size effect on IMC growth. Park et al. [1] investigate the interfacial reaction of Sn1.0Ag0.5Cu (SAC105) solder ball joints with diameter from 200 to 400 μm . They concluded that the Cu_6Sn_5 IMC thickness increased as the solder ball size decreased. Chol et al. [2] used the Tin-plated Cu balls to study the solder volume effect on interfacial reaction. They found that the IMC growth rate of 10 μm Sn on Cu balls was much larger than that of 40 μm Sn on Cu ball. When the Sn layer decreased to 5 μm , the IMC volume became much smaller than other samples. The results suggested that IMC thickness not always increased with the decreasing of solder volume.

Chang et al. [3] performed a comprehensive study on the effect of solder volume on consumption of Cu pad by using lead-free solder with different Cu concentration. Based on the Cu consumption rate, they conclude that the Cu_6Sn_5 intermetallic size increases with decreasing of solder volume. It is well known that under soldering or thermal aging, part of the Cu substrate is consumed to form the IMC at the

✉ Yao Yao
yaoy@nwpu.edu.cn; yaooay@gmail.com

¹ School of Mechanics, Civil Engineering and Architecture, Northwestern Polytechnical University, Xi’an 710072, People’s Republic of China

interface and inside the solder joint. The interfacial IMC layer could have more serious influence on the solder joint reliability than IMC inside the joints. However, previous researches on size effect of interfacial reaction of solder joints mainly focus on the total Cu consumption. The size effect of solder joints on interfacial IMC layer is still lack of convincing data. The relationship between IMC growth rate and joint size still requires further research.

Besides interfacial IMC layer, tensile strength is another vital factor that influences the solder joints reliability. There are many studies with regard to the size effect on mechanical property of solder interconnects, which mainly focused on the ultimate tensile strength and constraint effect of solder joints [4–10]. Yin et al. [4] analyzed the tensile strength of solder joints with different diameters based on the Bridgman's theory, and found an inverse proportion relation between the tensile strength and the volume of solder joints. The ultimate tensile strength of Sn3.0Ag0.5Cu solder joint with thickness of 75 μm was 110 MPa, which was about three times of the yield stress. Qin et al. [5] revealed the fracture behavior and constraint effect of Ni/Sn3.0Ag0.5Cu/Ni solder joints by using finite element method. Besides, the tensile strength of Ni/SAC/Ni solder joints was found to be higher than Cu/SnAgCu/Cu solder joints with the same size. Wang et al. [6] studied the ductile–brittle transition of solder joints with different sizes, the reverse proportion relationship between the volume and tensile strength was observed in the experiments. However, most of the relations between solder volume and tensile strength are empirical formula.

Even though some pioneer works have been performed in the previous research, the size effect of solder joint on microstructure and mechanical properties is still unclear. The damage initiation and propagation in solder joints are related to IMC thickness [11], solder joint with thinner IMC layer tends to have ductile fracture while thicker IMC leads to brittle fracture. The ductile–brittle transition is contributed by not only stress triaxiality but also interfacial microstructure formation and growth. The IMC inside the solder joints are found to be one of the sources of micro-crack or micro-void when the joints are under tensile load [12]. The prism Cu_6Sn_5 inside solder joints can also deteriorate the ductility. Therefore, the size effect of solder joints is quite complex and the physical mechanism still requires further investigation.

In this work, different sizes of Cu-substrate Sn3.0Ag0.5Cu solder joints were made in lead-free solder soldering machine. The diameter of solder joints are 2 mm with the thickness ranges from 50 μm to 2 mm. Both interface and solder alloy microstructure of the joints are analyzed based on the scanning electron microscope images. The size effect coupled with thermal aging effect on IMC thickness and morphology are investigated. The ultimate tensile strength of Cu-substrate Sn3.0Ag0.5Cu solder joints is measured and

the -field based fracture criterion is employed to predict the tensile strength of solder joints with different sizes.

2 Experimental procedure

Different sizes of line-type solder joints were made through soldering process, which is widely adopted in electronic packaging producing. To guarantee the line-type solder joints have proper tensile property, the 2 mm diameter cylindrical Cu bar at both ends were fine polished, and then aligned in the quartz glass with V-groove. Before the soldering procedure, both cylindrical Cu ends were covered with flux, then Sn3.0Ag0.5Cu solder films with different thickness were set between the two ends. Figure 1a shows a regular temperature curve of lead-free solder soldering procedure. The quartz glass was put in T200N Lead-free Reflow *H* Soldering Machine, as shown in Fig. 1b. After soldering, the quartz glass was put in ultrasonic wave machine to remove the residual flux. The thickness of Sn3.0Ag0.5Cu solder joints after soldering ranges from 50 μm to 2 mm, as shown in Fig. 1c. The microstructure of solder joint was observed under scanning electron microscope (SEM), and size effect on microstructure of the solder joints as soldering was analyzed.

The effects of temperature on microstructure especially interfacial structure of Cu-substrate Sn3.0Ag0.5Cu solder joints were experimentally investigated. Solder joints with different sizes were put in a temperature chamber for thermal aging at 210 and 300 $^{\circ}\text{C}$, which could represent both solid-state and liquid-state annealing. The aging time was from 6 to 96 h at 210 $^{\circ}\text{C}$ and 3 h at 300 $^{\circ}\text{C}$. The ultimate tensile strength of solder joints with different sizes were measured by using BOSE EF3330 test system. For line-type solder joint, it is convenient to perform tensile tests but difficult to measure the true elongation. Previous researches usually took the grip displacement as the elongation of solder joints, which could also include the elongation of substrate. To capture the relatively accurate elongation of solder joint, extensometer gauge with measuring range of 10 mm was adopted in the tensile test. Tensile strain can be calculated by gauge elongation divided by the thickness of solder joints. The tensile stress was measured by tensile load divided by the cross section area of solder joints.

3 Results and discussion

3.1 Interfacial IMC growth of different sizes solder joints

Microstructure of solder joints has essential influence on mechanical property. Determination of solder joints

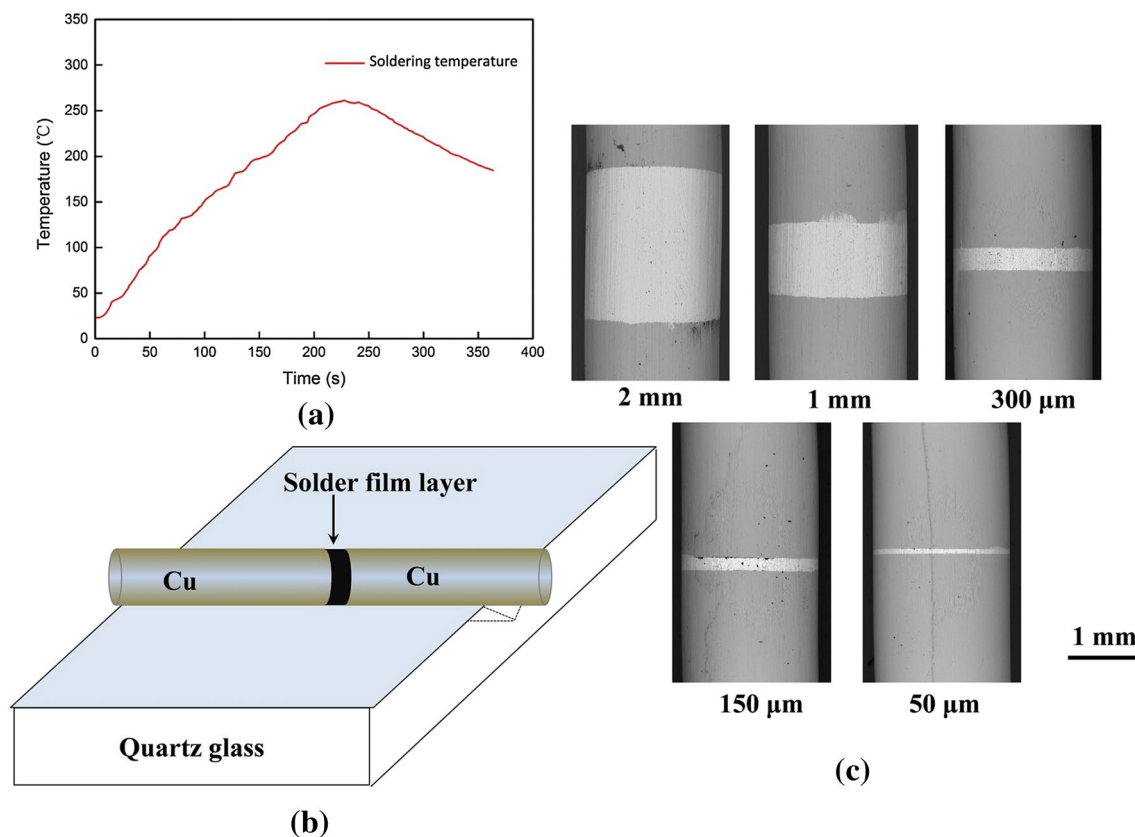


Fig. 1 **a** Soldering temperature curve; **b** Schematic of quartz glass with V-groove; **c** representative solder joints with different sizes

reliability also requires the understanding of interfacial reaction and intermetallic growth, the interfacial intermetallic growth mechanism of lead-free solder joint was summarized in [11, 13, 14]. For Cu-substrate solder joints, Cu_6Sn_5 intermetallic layer forms during soldering procedure and continuously grow in the service life. Under soldering or annealing condition at elevated temperatures, Cu_3Sn intermetallic forms between Cu_6Sn_5 and substrate through consuming parts of Cu_6Sn_5 and Cu substrate. Based on the classic Lifshitz–Slezov–Wagner (LSW) theory [13], the driving force of IMC layer growth comes from the decreasing of surface area. Thus, the scallop-type intermetallic will transfer to lamellar-type which possesses a smaller surface area. For an open system where the Cu substrate continuously supply the interfacial reaction, Gusak and Tu [13] proposed a flux-driven ripen theory. Their theory assumes that the shape of scallop-type intermetallic is hemisphere and the total surface area keeps constant while the total volume of the intermetallic increases. The driving force comes from free energy releasing during IMC layers growth. Each theory has its own hypothesis and valid under specific conditions.

With the development of 3D integrated circuit technology, the size of solder joint decreases from 200 μm to sub-50 μm . In the current research, the micro structure of IMC

layers of Sn3.0Ag0.5Cu solder joints with different sizes is investigated. The size effect of solder joints on interfacial structure is taken into account. It is found that the intermetallic thickness is associated with solder joints sizes. The SEM image of interfacial microstructure of Sn3.0Ag0.5Cu solder joints with thickness ranges from 50 μm to 2 mm are shown in Fig. 2. All the IMC of five solder joints sizes are scallop-type, the average IMC thickness generally increases for thicker solder. The average IMC thickness of 50 μm thick solder is 2.58 μm while the IMC of 2 mm thickness solder grows to 4.59 μm , as show in Fig. 3.

The size effect of solder joints on IMC thickness used to be ignored, however, the current experimental results show that the interfacial IMC thickness decreases as the size of solder joints decreases, which could play an important role in the solder reliability. Current results also show that the size of Cu_6Sn_5 grains in IMC layer increase with solder joints thickness decrease. The results are in according with observation by Huang et al. [8].

The size effect on IMC thickness of solder joints shows that the IMC growth rate varies as a function of the joint size. To further prove the observation, the interfacial structure of solder joints with different sizes after thermal aging is investigated. SEM images of interfacial microstructure

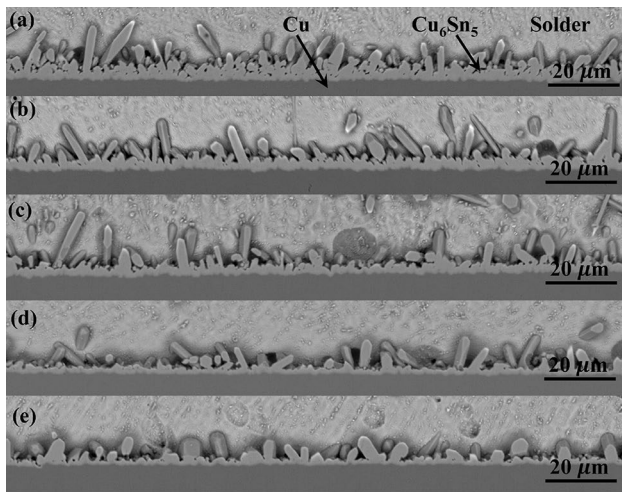


Fig. 2 SEM image of interfacial microstructure of Sn3.0Ag0.5Cu solder joint with different sizes as soldering, **a** 2 mm thickness, **b** 1 mm thickness, **c** 300 μm thickness, **d** 150 μm thickness, **e** 50 μm thickness

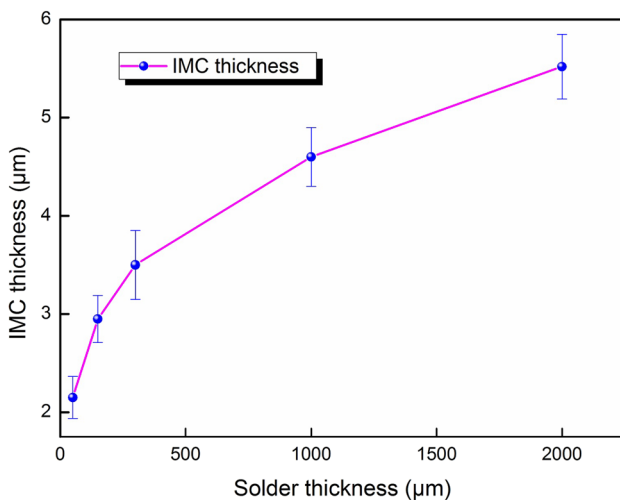


Fig. 3 IMC thickness of Sn3.0Ag0.5Cu solder joint with different sizes as soldering

of solder joints after 210 °C of thermal aging for 6, 24, and 96 h are shown in Fig. 4a–c. The size of solder joints from top to bottom in Fig. 4a–c is 2 mm to 50 μm, in the same sequence with Fig. 2. The relationship between IMC thickness and thermal aging time is summarized in Fig. 4d. Before thermal aging, the IMC structure is composed of slanting Cu₆Sn₅ prisms (Fig. 2). After thermal aging for 6 h at 210 °C, the IMC of solder joint with thickness of 50 and 150 μm transforms to lamella-type and the slanting Cu₆Sn₅ prisms disappears. For 300 μm to 2 mm thickness solder joints, the slanting Cu₆Sn₅ prisms IMC transforms to scallop-type (Fig. 4a). After 96 h of thermal aging at 210 °C,

scallop-type IMC in 300 μm to 2 mm thickness solder joints transformed to lamella-type, while the lamella-type IMC of 50 μm and 150 μm thickness solder joints kept lamella and grew to 9 μm (Fig. 4c).

It is interesting to note that although the IMC of smaller size solder joints is thinner than larger size solder joints, the IMC of all solder joints approximately grows to the same thickness (about 9 μm) after thermal aging for 96 h at 210 °C. The Cu₃Sn layer was not obviously observed after 210 °C thermal aging for 6 h. As thermal aging time increased to 24 h, Cu₃Sn layer grew to 1.1 μm, and when thermal aging increased to 96 h, Cu₃Sn layer grew to 1.9 μm. In general, the size effect on the growth rate of Cu₃Sn layer after 210 °C thermal aging is not pronounced, and the thickness of Cu₃Sn layer is much thinner compared with Cu₆Sn₅. The relationship between IMC thickness and aging time generally follows the Fick’s law:

$$h = \sqrt{Dt} \tag{1}$$

where *h* is the average IMC thickness and *t* is the aging time, *D* represents the growth rate which can be determined by the slope of the line in *h* versus \sqrt{t} , as shown in Fig. 4d.

The IMC growth rate of solder joints decreases as the joint thickness increases under thermal aging at 210 °C, as show in Fig. 5, that means the IMC layer of larger solder joint grows faster than smaller solder joint. If the growth rate of IMC during soldering also matches this relation, larger solder joints should possess thicker intermetallic layer. However, the IMC thickness of solder joints as soldering does not support this inference. Thus, the relationship between IMC growth rate and solder joint size should be different during soldering procedure and thermal aging. The above analysis shows that solder joint size has pronounced effect on interfacial microstructure in both liquid-state reaction and solid-state thermal aging. The major difference between soldering and 210 °C thermal aging is of solder phase state. Under soldering procedure, IMC grows between liquid solder and Cu substrate, while under thermal aging the interfacial reaction is at solid state.

Because channel assisted Cu flux drives IMC thickness increasing while ripening flux transforms the flatness of IMC layer, current results show that both ripening flux and the channel assisted Cu flux contributed to the IMC growth in the thermal aging process. The channel assisted Cu flux rate during the early 24 h is higher than the later 72 h.

It is reasonable to conclude that the IMC in smaller size solder joints grows slower than in larger size under liquid-state interfacial reaction, while IMC in smaller size solder joints grows faster than in larger size under solid-state interfacial reaction. To further verify the conclusion, liquid-state thermal aging tests with different sizes of Sn3.0Ag0.5Cu solder joints were conducted for 2 h at 300 °C. Under 300 °C thermal aging condition, the IMC growth is also

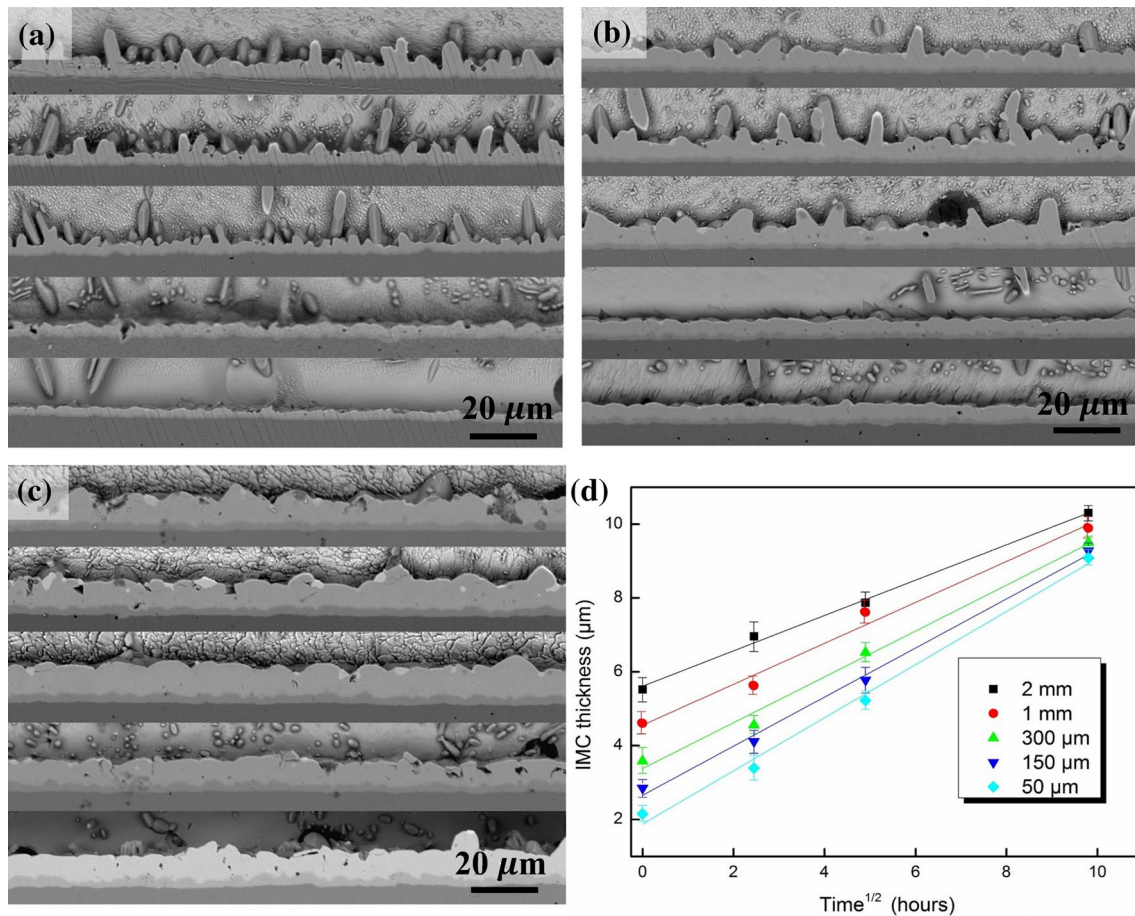


Fig. 4 **a** SEM image of interfacial microstructure of Sn3.0Ag0.5Cu solder joint with different sizes after thermal aging for 6 h at 210 °C, **b** thermal aging for 24 h, **c** thermal aging for 96 h; **d** average thickness of IMC layer of different sizes solder joints after thermal aging at 210 °C

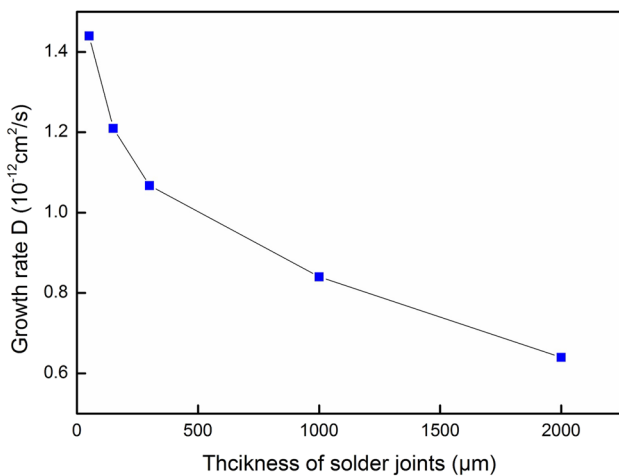


Fig. 5 The IMC growth rate of solder joint with different sizes under thermal aging at 210 °C

in liquid-state interfacial reaction as soldering procedure, except the temperature is elevated. Thus, the experimental results of 300 °C liquid-state thermal aging can be applied to validate the conclusion (Fig. 6).

The SEM image of interfacial structure of solder joints after 300 °C thermal aging is shown in Fig. 7. The average and the IMC thickness of solder joints as soldering is also given in Fig. 8 by double Y axial plot. It is clearly shown that IMC thickness after 300 °C thermal aging is much thicker than IMC of solder joints as soldering, and the two curves exhibit similar relationship between IMC and solder joints thickness. When the thermal aging temperature is elevated, it is observed that the IMC grows much faster than thermal aging at 210 °C.

Along with the similar IMC thickness growth trend, there are some morphology and composition differences between the interfacial structure after soldering and thermal aging at 300 °C. The IMC of solder joints after soldering is composed of Cu_6Sn_5 , while most of the IMCs are Cu_3Sn after 300 °C thermal aging. During the soldering procedure, both solid and liquid states are included and the IMC layer can

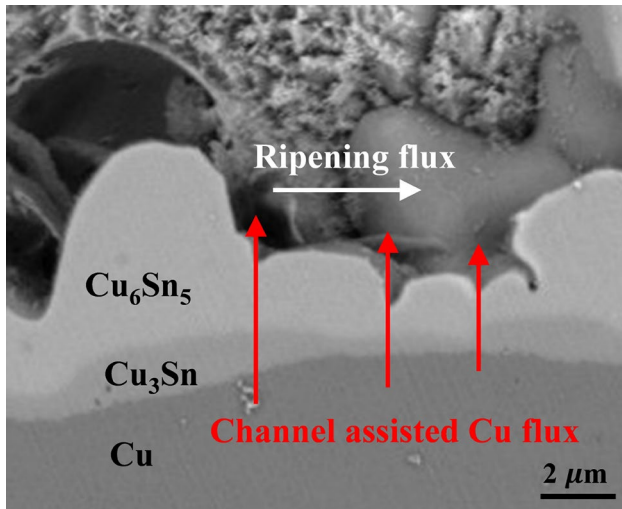


Fig. 6 Schematic diagram of channel assisted Cu flux and ripening flux

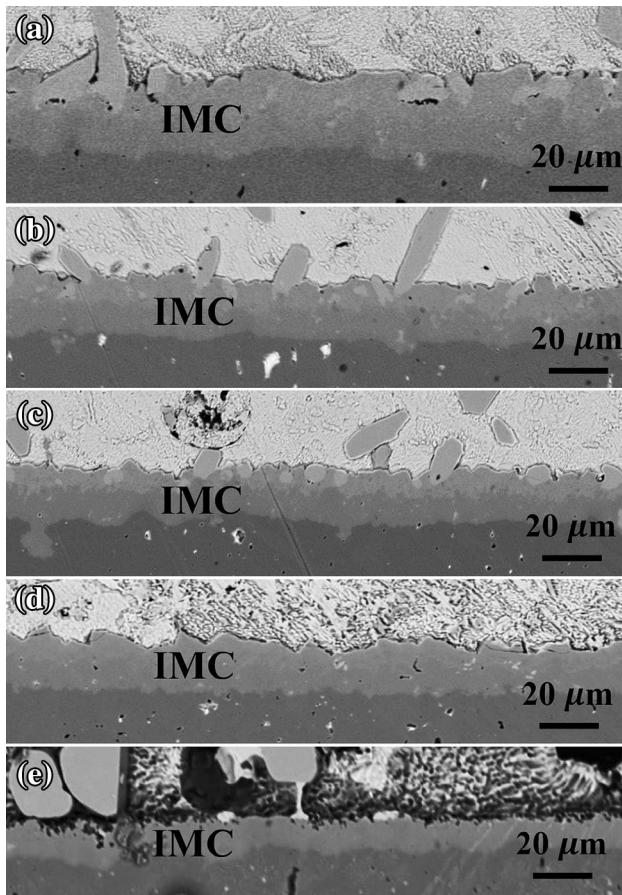


Fig. 7 Intermetallic structure of Cu-substrate after 300 °C thermal aging for 2 h. The thickness of the joints are **a** 2 mm, **b** 1 mm, **c** 300 μm, **d** 150 μm, **e** 50 μm

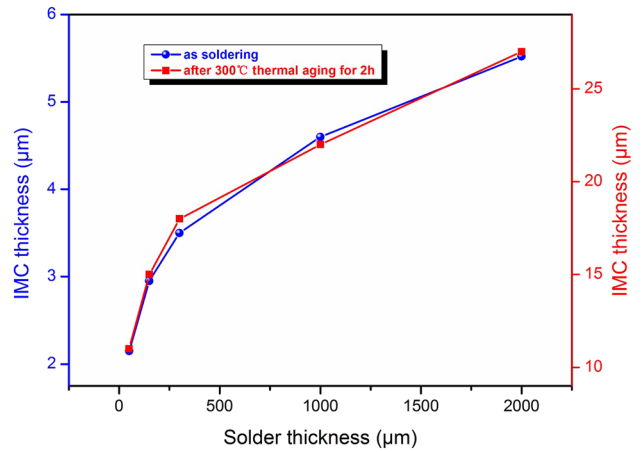


Fig. 8 The IMC thickness of Sn3.0Ag0.5Cu solder joints after thermal aging at 300 °C for 2 h compared with IMC thickness of Sn3.0Ag0.5Cu solder joints as soldering

grow during both states. It is noted that the IMC growth rate during liquid state is much higher than solid state, as shown in Fig. 8. Thus, it is reasonable to compare the IMC thickness of solder joint as soldering and after thermal aging. The morphology of IMC after soldering is slanting Cu_6Sn_5 prisms while the IMC becomes lamella-type after 300 °C thermal aging. Even though after thermal aging the IMC structure is quite different from that after soldering, the IMC thickness shows similar relation with solder joint thickness, which verifies that the IMC thickness is dependent on solder joint size, and smaller size joint possesses slower interfacial reaction rate in liquid-state thermal aging but faster interfacial reaction in the solid-state thermal aging.

The size effect not only exists at the interfacial IMC layer, but also being observed in microstructure of solder. Figure 9 shows the SEM image of solder joints microstructure. Different morphologies of Cu_6Sn_5 intermetallic compound are observed to be related to the solder joints size. In the 2 mm thickness solder joint, ‘H’ type prism Cu_6Sn_5 can be observed, as shown in Fig. 9a. The image in the solid black box of Fig. 9a is the shrink of ‘H’ type prism. This type of prism is typically found in Sn3.0Ag0.5Cu solder joints after soldering [15]. Inside 1 mm thickness solder joint, hollowed hexagonal prisms Cu_6Sn_5 is found instead of ‘H’ type Cu_6Sn_5 prisms. The image in the solid black box in Fig. 9b shows the shrink of hollowed hexagonal prism Cu_6Sn_5 . As the solder joint thickness reduces to 300 μm, the dimension of hexagonal Cu_6Sn_5 prisms becomes smaller than that in 1 mm thickness. When solder joint thickness reduces to 150 μm, the cross section of Cu_6Sn_5 prisms inside the joints is even smaller and the hexagonal Cu_6Sn_5 prism is not observed. When solder joints thickness reduces to 50 μm, there is no observable Cu_6Sn_5 intermetallic compound inside the joints.

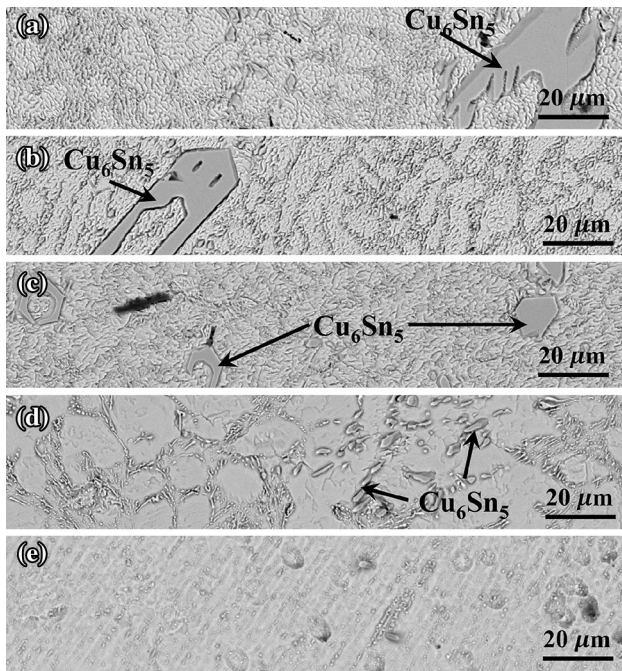


Fig. 9 SEM images of Sn3.0Ag0.5Cu solder joints, **a** 2 mm thickness, **b** 1 mm thickness, **c** 300 μm thickness, **d** 150 μm thickness, **e** 50 μm thickness

Hexagonal Cu_6Sn_5 prism is one of the damage initiation positions under tensile loading. Sn3.0Ag0.5Cu solder behaves ductile while Cu_6Sn_5 is quasi-brittle, which can cause incompatible deformation. It is noted that larger solder joints contain more hexagonal Cu_6Sn_5 , micro crack tends to initiate when Cu_6Sn_5 prism breaks. For Cu-substrate Sn3.0Ag0.5Cu solder joints, the formation of interfacial Cu_6Sn_5 IMC layer consumes not only Cu in substrate but also Cu inside the joints. When the solder joint thickness reduces to 50 μm , most of the Cu in solder joints is consumed by interfacial Cu_6Sn_5 formation, little quantity of Cu is left for Cu_6Sn_5 forming inside joints.

3.2 Tensile test of solder joints with different sizes

With the development of 3D chip integration, the size of solder interconnects gets smaller, micro-bump size even reduces to below 20 μm [16]. It is observed that the grains in 50 μm thickness solder joints after thermal aging can be coarsen to 30 μm , which means the micro-bump might be consisted of a few or only single grain. Thus, the mechanical and thermal properties of micro-bump are dependent on the statistical orientation of solder grains. This statistical orientation property may affect the tensile strength of solder joints with different sizes.

Line-type solder joints with a diameter of 2 mm and thickness varies from 2 mm to 50 μm were prepared to

measure the tensile property of solder joints. Stress–strain curves of solder joints with thickness of 2, 1 mm, 300, 150, 50 μm are shown in Fig. 10, which clearly exhibits a ductile to brittle transition. For solder joints with thickness of 2 and 1 mm, the stress–strain curves show low tensile strength but good ductility. For solder joints with thickness of 50 to 300 μm , the tensile procedure shows higher tensile strength but relative brittleness. The horizontal parts of stress–strain curve represents the elongation of solder after it reaches the maximum tensile stress. The horizontal part of stress–strain curves gets shorter with thinner solder joint. At the end of horizontal parts with the thickness of 50, 150, and 300 μm , there is no descending phase because the crack in solder joint develops too fast to catch stress-dropping.

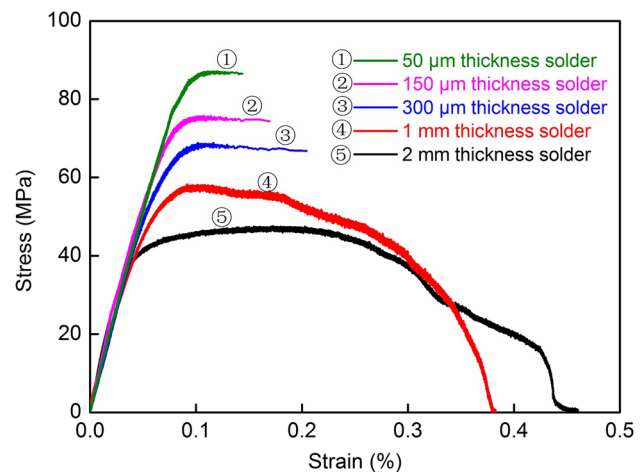


Fig. 10 Stress strain curve of brass-substrate solder joint with different sizes

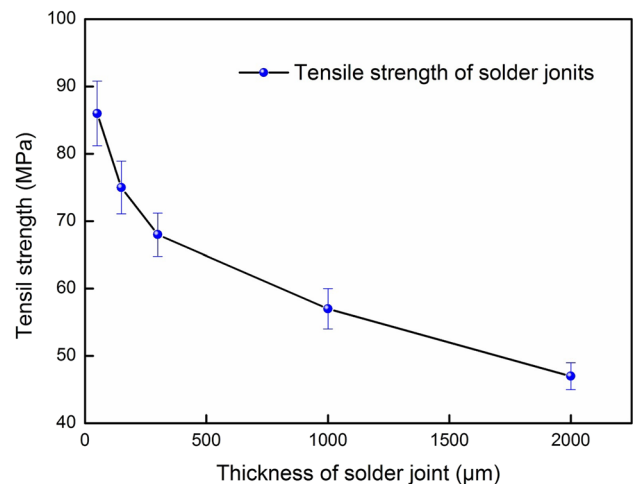


Fig. 11 Tensile strength of Cu-substrate solder joints with different sizes

Ten solder joint specimens for each thickness were tested to obtain the average tensile strength of different sizes, the standard deviation is within ± 4.8 MPa as shown in Fig. 11.

3.3 Fracture characteristic of solder joints with different size

Compared with conventional Sn-Pb solder, Sn-Ag-Cu solder alloy possess higher tensile strength, meanwhile the introduction of Ag and Cu may contribute to brittle IMC at both interface and inside the joints. The decreasing of ductility aggravates the solder joint failure induced by thermal stress, and brings the interfacial failure [17–20]. As shown in Fig. 12, micro-crack or micro-void tends to initiate at the interface of solder joints. To probe into the ductile–brittle transition mechanism induced by decreasing of joint size, the fracture characteristics of solder joints with different sizes are analyzed from both macro and micro point of view. Both ductile and quasi-brittle fracture types are observed in the experiments, different fracture types are found corresponding to the size of solder joints.

In general, the stress–strain curve can be divided into three stages. The first stage is elastic phase, which has no plastic damage. The second stage is the plastic phase, micro-damage such as dislocation and micro-crack initiated before reaching the ultimate tensile stress, then the micro-cracks start to grow. The last stage is the descending phase, micro-cracks and voids coalesced until final rupture. For solder joints with thickness of 2 and 1 mm, fracture is initiated from the corner of solder joints and near the intermetallic layers, as shown in Fig. 13. After initiating at the corner, the fracture front becomes blunted due to plastic flow and can store more strain energy. As the tensile load increases, the plastic zone keeps expanding and crack tip moves forward. The fracture is not always moving along the intermetallic layer, sometimes it can be controlled by the shear plane.

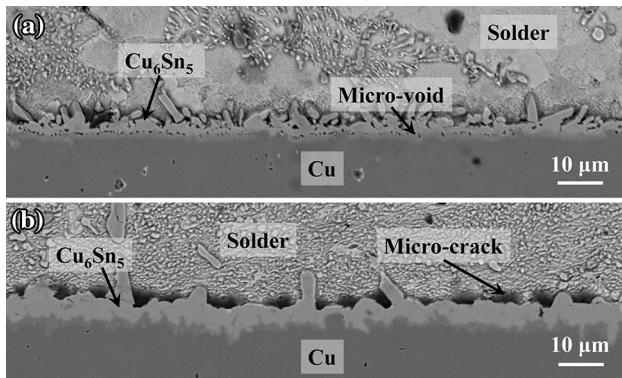


Fig. 12 Micro-void and micro-crack initiated at the interface of a $\text{Cu}_6\text{Sn}_5/\text{Cu}$, b solder/ Cu_6Sn_5

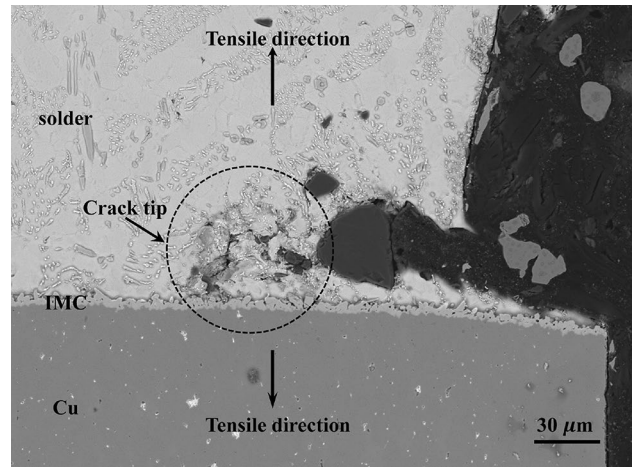


Fig. 13 fracture initiated from the corner of solder joints

Figure 14 shows the macro fracture morphology of solder joints with thickness of 2, 1 mm and 300 μm . The angle between shear plane and substrate is about 36° (Fig. 14a) and 52° (Fig. 14b) for solder joints with thickness of 2 and 1 mm, respectively. For solder joints with thickness from 300 to 50 μm , the fracture exhibits different characteristics. Micro-crack tends to initiate at the interfaces, then coalescing until the whole interface is tore apart. Because the solder layer is a thin film, the crack can easily breakthrough solder layer and reach the opposite side of intermetallic. Considering the crack evolution is too fast for the sensor to capture the load descending, only plastic phase of the stress–strain

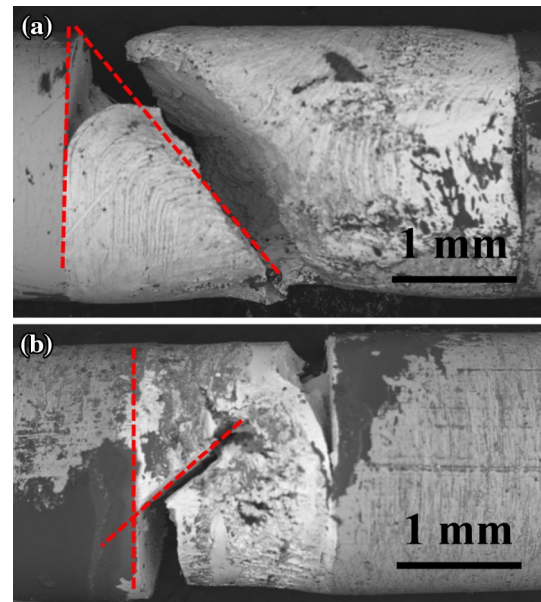


Fig. 14 Representative macroscopic fracture morphology after tensile test

Fig. 15 Fracture surface of 50 μm solder joint after tensile test

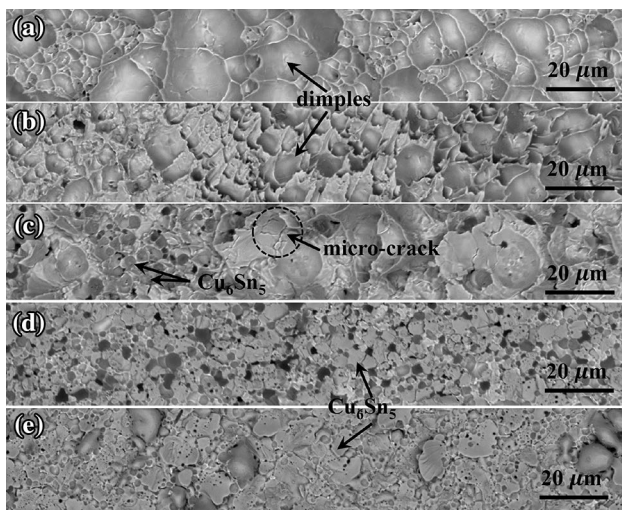
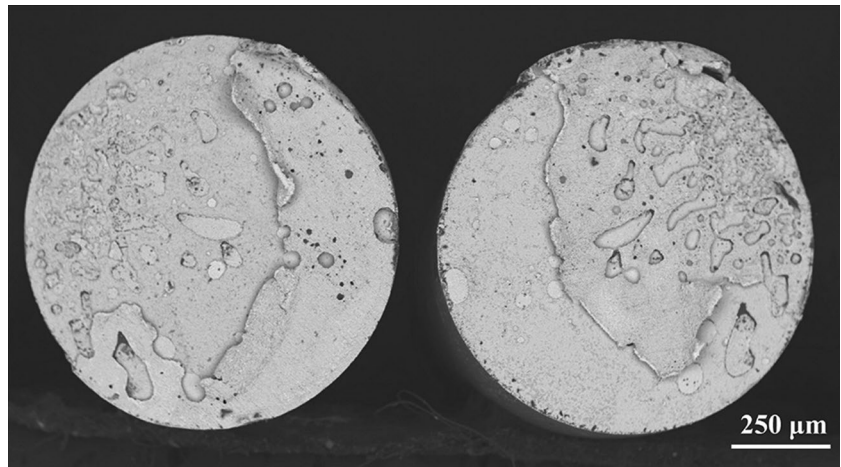


Fig. 16 SEM images of the fracture morphology of solder joint **a** 2 mm thickness, **b** 1 mm thickness, **c** 300 μm thickness, **d** 150 μm thickness, **e** 50 μm thickness

curves of 300 to 50 μm solder is shown without the descending phase. In Fig. 15, it shows that the crack surface is not a flat section but a peeling layer with many pits.

From the microstructure point of view, the fracture morphology is consistent with ductile–brittle transition, and the dimples are the characteristic of ductile fracture. Figure 16a shows the ductile fracture morphology of 2 mm solder joints. When the solder joint thickness drops to 1 mm, the dimple size decreases and density increases, as shown in Fig. 16b. When solder joint thickness decreases to 300 μm , there are only a few numbers of dimples. Among these dimples, micro-cracks can be observed in the cup-wall, as shown in Fig. 16c. At the bottom of dimples, Cu_6Sn_5 IMC is observed, which illustrates that the crack surface is close to the Cu_6Sn_5 IMC layer. The dimple morphology transition illustrates that decreasing of solder joints thickness restricts the plastic

deformation of solder. Thus it requires higher local stress to break the bonds, which raises the ultimate tensile strength. When the solder joint thickness decreases to 150 and 50 μm , fracture type turns to brittle. Dimple does not appear and the whole fracture surface is occupied by intergranular and transgranular fractured Cu_6Sn_5 , as show in Fig. 16d and e.

3.4 Predict the tensile strength with the H-field based fracture criterion

Both experimental and numerical analysis illustrate that there exists stress singularity zone at the interface corner of sandwich-type solder joint. Therefore damage tends to initiate at the corner, as shown in Fig. 13. During the past decades, researches with respect to adhesive joint have provided clearly understanding on the interface stress singularity, and several of fracture criteria have been developed for bonded joint structure [21–23]. The fracture criteria proposed by Akisanya and Meng [23] is based on the connection of stress field and the interface corner stress intensity factor, also called H field. In the linear elastic fracture domain, the stress near the corner of interface can be given in the form of $Hr^{\lambda-1}$, where r is the radial distance from the corner and $\lambda - 1$ is the singularity order which is defined in [24]. This fracture criterion states that fracture initiates when the interface corner stress intensity factor H reaches the critical value H_c . The criteria is valid when the fracture zone or non-linear deformation district is inside the H field domain. In the current study, the H_c fracture criterion is adopted to predict the ultimate tensile strength of solder joints with different thickness.

Considering a sandwich-type solder joint, the joint is subjected to a uniaxial tensile load in the X direction. Then the asymptotic stress field solution is given as [23]:

$$\sigma_{ij} = Hr^{\lambda-1}f_{ij} \quad (2)$$

where f_{ij} is non-dimensional function dependent on α , β and θ , the parameter i and j are plane polar coordinates. In this case, $(i, j) \equiv (r, \theta)$. Under the plain strain condition, α and β are given in the following form [15]:

$$\alpha = \frac{(1 - \nu_2)/\mu_2 - (1 - \nu_1)/\mu_1}{(1 - \nu_2)/\mu_2 + (1 - \nu_1)/\mu_1} \tag{3}$$

$$\beta = \frac{1}{2} \frac{(1 - 2\nu_2)/\mu_2 - (1 - 2\nu_1)/\mu_1}{(1 - \nu_2)/\mu_2 + (1 - \nu_1)/\mu_1}$$

where ν_1 and ν_2 are Poisson’s ratio of brass and solder, respectively, μ_1 and μ_2 are shear modulus of substrate and solder. The intensity factor H in Eq. (1) is defined as:

$$H = \sigma h^{\lambda-1} Q(\alpha, \beta) \tag{4}$$

where σ is the remote tensile stress, h is the thickness of solder layer, the non-dimensional constant function Q is dependent on the material parameters α and β . The value of Q and stress singularity parameter λ is obtained from the analysis in [25–28]. Elastic modulus of Cu is 110 GPa, the Poisson’s ratio is 0.31, and the shear modulus is 42 GPa. For Sn3.0Ag0.5Cu, elastic modulus is 34.5 GPa, the Poisson’s ratio is 0.37, and the shear modulus is 12.6 GPa. Therefore, $\alpha = 0.51$, $\beta = 0.087$, $\lambda = 0.873$, $Q = 0.71$. For solder joint with 1 mm thickness, the failure stress is $\sigma_f = 57$ MPa, thus $H_C = \sigma h^{1-\lambda} Q = 40.5$. The failure stress of solder joint of different thickness can then be determined if H_C is a valid fracture parameter. The predictions by H field fracture criterion are compared with experimental data in Fig. 17, which shows reasonable accuracy.

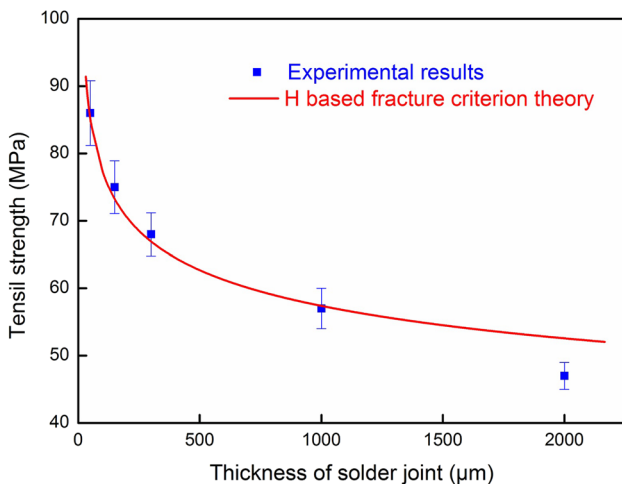


Fig. 17 Tensile strength of Sn3.0Ag0.5Cu solder joints predicted by the H-field fracture criterion compared with experimental results

4 Conclusion

In the current study, the size effect of Sn3.0Ag0.5Cu solder joints on interfacial IMC layer and Cu₆Sn₅ intermetallic compound are investigated experimentally.

- (1) The IMC layer thickness of solder joints is found to be dependent on the joints thickness. The IMC thickness of smaller size solder joint (50 µm thickness) is 2.58 µm while the IMC of larger size solder joint (2 mm thickness) is 4.59 µm after soldering.
- (2) The effects of solid-state at 210 °C and liquid-state thermal aging at 300 °C on IMC thickness are investigated. The average IMC thickness of solder joints after thermal aging for 2 h at 300 °C are much thicker than joint as soldering, but the tendency between IMC thickness and solder joint thickness is approximately the same. For solid-state thermal aging at 210 °C, the IMC in smaller size solder joint grows faster than larger size one, while under liquid-state thermal aging at 300 °C, the IMC growth rate in smaller size solder joint is slower than larger size one.
- (3) Size effect of solder joints on intermetallic compounds inside joints is observed. ‘H’ type prism Cu₆Sn₅ and hexagonal prism Cu₆Sn₅ are found in 2 mm thickness solder joint while only hexagonal prism Cu₆Sn₅ can be found in 1 mm and 300 µm thickness solder joints. As the solder joint thickness reduces to 50 µm, few Cu₆Sn₅ IMC can be found inside the solder joint.
- (4) Tensile strength of solder joints with thickness ranging from 2 mm down to 50 µm is measured. The tensile strength ranges from 42 MPa to 93 MPa and the solder joints of different thickness show a ductile–brittle transition.
- (5) H-field based fracture criterion theory is employed to predict tensile strength of different thickness solder joints, which shows reasonable accuracy compared with experimental results.

Acknowledgements This work was supported by the National Natural Science Foundation of China (No. 11572249 and 51508464). This work was also partially supported by “the Fundamental Research Funds for the Central Universities” (No. 3102016ZY017).

References

1. Y.S. Park, Y.M. Kwon, J.T. Moon, Y.W. Lee, Effects of fine size lead-free solder ball on the interfacial reactions and joint reliability. in *Proceedings of Electronic Components and Technology Conference*, (IEEE, 2010) pp. 1436–1441.
2. W.K. Choi, S.K. Kang, D.Y. Shih, A study of the effects of solder volume on the interfacial reactions in solder joints using the

- differential scanning calorimetry technique. *J. Electron. Mater.* **31**(11), 1283–1291 (2002)
3. C.C. Chang, Y.W. Lin, Y.W. Wang, C.R. Kao, The effects of solder volume and Cu concentration on the consumption rate of Cu pad during reflow soldering. *J. Alloys Compd.* **492**, 99–104 (2010)
 4. L.M. Yin, X.P. Zhang, C. Lu, Size and volume effects on the strength of microscale, lead-free solder joints. *J. Electron. Mater.* **38**(10), 2179–2183 (2009)
 5. H.B. Qin, X.P. Zhang, M.B. Zhou, J.B. Zeng, Y.W. Mai, Size and constraint effects on mechanical and fracture behavior of microscale Ni/Sn3.0Ag0.5Cu/Ni solder joints. *Mat. Sci. Eng. A* **617**(1), 14–23 (2014)
 6. Y. Wang, I.M. De Rosa, K.N. Tu, Size effect on ductile-to-brittle transition in Cu-solder-Cu micro-joints. *IEEE Electronic Components and Technology Conference* 632–639 (2015)**
 7. P. Zimprich, U. Saeed, A. Betzwar-Kotas, Mechanical size effects in miniaturized lead-free solder joints. *J. Electron. Mater.* **37**(1), 102–109 (2008)
 8. M.L. Huang, F. Zhang, F. Yang, N. Zhao, Size effect on tensile properties of cu/sn-9zn/cu solder interconnects under aging and current stressing. *J. Mater. Sci.* **26**(4), 1–8 (2015)
 9. K.S. Kim, S.H. Huh, K. Suganuma, Effects of intermetallic compounds on properties of Sn–Ag–Cu lead-free soldered joints. *J. Alloy Compd.* **352**(1–2), 226–236 (2003)
 10. Y.D. Han, H.Y. Jing, S.M. Nai, L.Y. Xu, C.M. Tan, J. Wei, Interfacial reaction and shear strength of Ni-coated carbon nanotubes reinforced Sn–Ag–Cu solder joints during thermal cycling. *Intermetallics* **31**(12), 72–78 (2012)
 11. T. An, F. Qin, Relationship between the intermetallic compounds growth and the microcracking behavior of lead-free solder joints. *J. Electron. Packag.* **138**(1), 011002 (2016)
 12. Y. Yao, R. An, X. Long, Effect of electric current on mechanical behaviour of Sn-Ag-Cu solder joints. *Eng. Fract. Mech.* **171**, 85–97 (2017)
 13. A.M. Gusak, K.N. Tu, Kinetic theory of flux-driven ripening. *Phys. Rev. B* **66**(11), 115403 (2002)
 14. G. Zeng, S. Xue, L. Zhang, L. Gao, W. Dai, J. Luo, A review on the interfacial intermetallic compounds between Sn–Ag–Cu based solders and substrates. *J. Mater. Sci.* **21**(5), 421–440 (2010)
 15. Y. Tian, R. Zhang, C. Hang, L. Niu, C. Wang, Relationship between morphologies and orientations of Cu₆Sn₅ grains in Sn_{3.0}Ag_{0.5}Cu solder joints on different Cu pads. *Mater Charact* **88**(2), 58–68 (2013)
 16. K.N. Tu, Reliability challenges in 3D IC packaging technology. *Microelectron. Reliabil* **51**(3), 517–523 (2011)
 17. Y. Yao, L.M. Keer, M.E. Fine, Modeling the failure of intermetallic/solder interfaces. *Intermetallics* **18**(18), 1603–1611 (2010)
 18. Y. Yao, L.M. Keer, Cohesive fracture mechanics based numerical analysis to BGA packaging and lead free solders under drop impact. *Microelectron. Reliabil.* **53**(4), 629–637 (2013)
 19. SPV Nadimpalli, J.K. Spelt, Fracture load prediction of lead-free solder joints. *Eng. Fract. Mech.* **77**(17), 3446–3461 (2010)
 20. X. Hu, T. Xu, L.M. Keer, Y. Li, X. Jiang, Shear strength and fracture behavior of reflowed Sn_{3.0}Ag_{0.5}Cu/Cu solder joints under various strain rates. *J. Alloy Compd.* **690**, 720–729 (2017)
 21. Y. Suzuki, Adhesive tensile strengths of scarf and butt joints of steel plates (relation between adhesive layer thicknesses and adhesive strengths of joints): solid-mechanics, strength of materials. *Nihon Kikai Gakkai Ronbunshu A Hen/Trans. Jpn. Soc. Mech. Eng. A* **53**(487), 514–522 (1987)
 22. G.C. Sih, J.W. Ho, Sharp notch fracture strength characterized by critical energy density. *Theor. Appl. Fract. Mech.* **16**(3), 179–214 (1991)
 23. A.R. Akisanya, C.S. Meng, Initiation of fracture at the interface corner of bi-material joints. *J. Mech. Phys. Solids* **51**(1), 27–46 (2003)
 24. D.B. Bogy, Two edge-bonded elastic wedges of different materials and wedge angles under surface tractions. *Int. J. Appl. Mech.* **38**(2), 377–386 (1971)
 25. D.B. Bogy, Edge-bonded dissimilar orthogonal elastic wedges under normal and shear loading. *Int. J. Appl. Mech.* **35**(3), 460 (1968)
 26. R.I. Babicheva, K.A. Bukreeva, S.V. Dmitriev, R.R. Mulyukov, K. Zhou, Strengthening of NiAl nanofilms by introducing internal stresses. *Intermetallics* **43**, 171–176 (2013)
 27. X. Long, Y.X. Wang, L.M. Keer, Y. Yao, Mechanical effects of isolated defects within a lead-free solder bump subjected to coupled thermal-electrical loading. *J. Micromech. Mol. Phys.* **1**, 165004 (2016)
 28. Z. Qian, A.R. Akisanya, An experimental investigation of failure initiation in bonded joints. *Acta Mater.* **46**(14), 4895–4904 (1998)